The computational study of the "inversion substitution" reactions CX3Br + O2 → CX3O2 + Br (X = H, F)

ARTICLE *in* COMBUSTION AND FLAME · JULY 2010

Impact Factor: 3.08 · DOI: 10.1016/j.combustflame.2009.11.004

3 AUTHORS, INCLUDING:

Anton S Nizovtsev
Nikolaev Institute of Inorganic Chemistry S…
10 PUBLICATIONS **20** CITATIONS
SEE PROFILE

Georgii A. Bogdanchikov
Russian Academy of Sciences
23 PUBLICATIONS **98** CITATIONS
SEE PROFILE

Combustion and Flame 157 (2010) 1382–1389

Contents lists available at ScienceDirect

Combustion and Flame

journal homepage: www.elsevier.com/locate/combustflame

The computational study of the "inversion substitution" reactions $CX_3Br + O_2 \rightarrow CX_3O_2 + Br$ (X = H, F)

Anton S. Nizovtsev [a,b,c], Georgii A. Bogdanchikov [a,b,c], Alexey V. Baklanov [a,b,*]

[a] Institute of Chemical Kinetics and Combustion, Institutskaya Str. 3, 630090 Novosibirsk, Russia
[b] Novosibirsk State University, Pirogova Str. 2, 630090 Novosibirsk, Russia
[c] Institute of Computational Mathematics and Mathematical Geophysics (Computing Center), Lavrentjev Ave. 6, 630090 Novosibirsk, Russia

ARTICLE INFO

Article history:
Received 18 September 2009
Received in revised form 9 November 2009
Accepted 10 November 2009
Available online 11 December 2009

Keywords:
Substitution reaction
Molecular oxygen
Bromine-containing fire suppressants
Quantum chemistry
Rate constants
Combustion

ABSTRACT

The kinetic parameters for the "inversion substitution" reactions of Br-containing fire suppressants CH_3Br and CF_3Br with molecular oxygen $CX_3Br + O_2 \rightarrow CX_3O_2 + Br$ (X = H, F) have been obtained on the basis of computational study carried out by quantum chemistry methods and transition state theory (TST). The DFT/B3LYP approach has been used to obtain molecular structures and vibrational frequencies and CCSD(T) method with additive corrections at MP2 and SODFT levels have been applied in order to calculate reaction enthalpies and activation barriers. Activation barrier for the substitution reaction $CH_3Br + O_2 \rightarrow CH_3O_2 + Br$ was found to be (53.3 kcal/mol) close to the endoergicity (51.2 kcal/mol) of bimolecular abstraction $CH_3Br + O_2 \rightarrow CH_2Br + HO_2$ which means that this "inversion substitution" should be considered as a competing process in the oxidation initiation of bromine containing substances. The results of these calculations together with the earlier results have allowed us to build the correlation of Evans–Polanyi type between the activation barrier and reaction enthalpy for "inversion substitution" reactions $CH_3X + O_2 \rightarrow CH_3O_2 + X$. For bromotrifluoromethane CF_3Br (Halon-1301) the barrier of "inversion substitution" was found to be of 86 kcal/mol that is higher by about 15 kcal/mol as compared with unimolecular decay $CF_3Br \rightarrow CF_3 + Br$ barrier. This makes negligible the role of bimolecular substitution reaction for kinetics of CF_3Br in oxygen environment. The TST calculations of the rate constants and their temperature dependence for the direct and reverse "inversion substitution" reactions have been carried out within the temperature interval of 273–2000 K.

1. Introduction

Chemical reactions of molecular oxygen with organic or inorganic substrates play a key role in combustion and atmospheric chemistry, oxidative biochemistry and chemical plant processes. The interaction of oxygen with substrate molecules results in the formation of free radicals which in turn propagate the chain oxidation process. For substrate molecules containing C–H, or generally X–H bonds, an abstraction reaction is supposed to be the initiation step. For example, in the process of oxidation of the saturated hydrocarbons RH, the generally accepted mechanism of initiation involves the reaction of hydrogen atom abstraction by molecular oxygen [1–4]:

$$RH + O_2 \rightarrow R + HO_2 \quad (1)$$

Recently, using a combination of quantum chemical calculations with G2M(CC,MP2) method and transition state theory (TST), we have studied the new class of bimolecular reactions of molecular oxygen $RH + O_2 \rightarrow RO_2 + H$ ($R = CH_3$, SiH_3) proceeding via the "inversion substitution" mechanism [5]. The results of these calculations allowed us to conclude that the "inversion substitution" reaction does not compete with the abstraction reaction (1) in the case of methane as a substrate. However, in the case of silane as a substrate ($RH = SiH_4$) the substitution reaction should contribute appreciably to the rate of initiation of homogeneous high-temperature oxidation of silane. The activation barrier for substitution reactions with the leaving group X

$$RX + O_2 \rightarrow RO_2 + X \quad (2)$$

should depend primarily on the bond strength of the broken bond R–X. We could thus expect a decrease in the barrier height for the case of a weaker bond with the leaving group X. This suggests that the role of "inversion substitution" reactions should increase for substrates RX where the R–X bond is weaker than the R–H bond. In agreement with this expectation it was shown within B3LYP/DZVP approach that for iodine atom as a leaving group in reactions $CH_3I + O_2 \rightarrow CH_3O_2 + I$ and $SiH_3I + O_2 \rightarrow SiH_3O_2 + I$ the barrier for substitution is lower than that for abstraction reactions by about

* Corresponding author. Address: Institute of Chemical Kinetics and Combustion, Institutskaya Str. 3, 630090 Novosibirsk, Russia. Fax: +7 383 3 30 73 50.
E-mail address: baklanov@kinetics.nsc.ru (A.V. Baklanov).

0010-2180/$ - see front matter © 2009 The Combustion Institute. Published by Elsevier Inc. All rights reserved.
doi:10.1016/j.combustflame.2009.11.004

20 kcal/mol and 8 kcal/mol, respectively [6]. In this paper we investigate the substitution reactions $CX_3Br + O_2 \rightarrow CX_3O_2 + Br$ (X = H, F) for substrates containing bromine atom as a leaving group. Bromine containing substances are often used as the fire suppressants [7,8]. Bromotrifluoromethane CF_3Br (Halon-1301) is one of the most effective flame inhibitors. One of the approaches used for the study of inhibitors efficiency is based on the calculations where the chemical kinetics is reproduced with the use of detailed chemical mechanism. This approach has been applied for investigation of both CH_3Br [9] and CF_3Br [9–12] efficiencies. This approach is often used also for the estimation of efficiency of alternative fire suppressants where CF_3Br is used as a benchmark [13]. In these studies the flame of methane in air is often used as a model. The addition of flame retardants always provides the increase in time of high-temperature reactions of methane in air but the effect of additives on the ignition delay can be of both signs [9]. The nature of this effect has been studied by Babushok et al. [9]. These authors have concluded that the effect of the additive on the ignition delay is governed by the initial retardant decomposition kinetics, which releases active species in the system. The mechanism used for the modeling of the inhibition effect of Br-containing fire suppressants involves the unimolecular decay $RBr \rightarrow R + Br$ as the step of initial retardant decomposition. In the case of CH_3Br the abstraction reaction of the type (1) should be considered as well. The substitution reaction of the type (2) also contributes to this initial kinetics of RBr retardants. It provides reactive species and so it can contribute to the promotion of combustion. The reverse process can be an effective chain termination step. So the kinetic parameters of substitution reactions are necessary to use in the modeling of combustion processes with RBr fire suppressants involved. In this work the necessary kinetic parameters are calculated as a result of computational study of these "new" substitution reactions $CX_3Br + O_2 \rightarrow CX_3O_2 + Br$ (X = H, F). The calculated parameters for the upper reactions together with the results obtained for the other substrates have been used to make the conclusions on the dependence of activation barrier upon the substrate structure and to obtain correlation between the barrier height and reaction enthalpy.

2. Computational details

Geometry of reactants, products and transition states (TSs) have been fully optimized using the hybrid density functional B3LYP method, *i.e.* Becke's three-parameter exchange functional [14] with the Lee–Yang–Parr correlation functional [15], with the all-electron Dunning's correlation-consistent polarized valence triple-zeta basis set augmented by diffuse functions, aug-cc-pVTZ [16–18] (AVTZ). All following single-point calculations were carried out with the B3LYP/AVTZ geometries.

Two levels of electronic structure theory, second-order Møller–Plesset perturbation theory (MP2) [19] and coupled-cluster method with single and double excitations and perturbative triples correction [CCSD(T)] [20,21], were applied for evaluation of electron correlation. Spin-unrestricted calculations were used for all open-shell systems.

The correlation of valence electrons was estimated at the CCSD(T)/AVTZ level within the frozen core (fc) approximation.

Core and core–valence correlation effects were calculated at MP2 level using the correlation-consistent polarized weighted core–valence triple-zeta (cc-pwCVTZ) [22,23] basis sets for C, F, O, Br atoms and AVTZ basis set for hydrogen atom. These effects were determined as the difference between the values obtained without (all-electron correlation, ae) and with frozen core approximation.

Scalar-relativistic effects were considered using a spin-free, one-electron Douglas–Kroll–Hess (DKH) [24–26] Hamiltonian with cc-pVTZ-DK [27] basis set intended for relativistic calculations. Scalar relativistic corrections were calculated as difference between MP2(DKH)/cc-pVTZ-DK and MP2/cc-pVTZ values.

Two-component spin–orbit density functional theory (SODFT) calculations have been carried out to estimate the spin–orbit coupling in open-shell transition states. As reported by Lee [28] spin–orbit coupling derived within SODFT formalism for molecules containing heavy elements are usually in a good agreement with those calculated within relativistic approaches of higher computational cost. In SODFT calculations we have also used B3LYP functional and AVTZ basis set for all atoms except bromine. For Br atom the shape-consistent relativistic effective core potential (RECP) with seven valence electrons generated by Christiansen and coworkers [29] and basis set of pVTZ quality specially optimized by Lee et al. [30] to work with this RECP were applied. A spin–orbit coupling was determined as difference between the relativistic effective potential (REP) and averaged REP (AREP) results calculated both on nonrelativistic B3LYP/AVTZ geometries and geometries optimized with inclusion of relativistic effects. For atomic Br the experimental value of spin–orbit coupling [31] was used.

Zero-point vibrational energies (ZPEs) were calculated with unscaled B3LYP/AVTZ harmonic vibrational frequencies. The thermal correction (TC) to the enthalpy has been calculated within rigid-rotor-harmonic-oscillator approximation. Deviation of $\langle S^2 \rangle$ value from 0.75 for doublet species and from 2.00 for triplet species was not significant in our calculations.

SODFT (REP and AREP) calculations were performed with the NWChem [32] program. All remaining calculations were carried out using Gaussian 03 [33] program package. Some basis sets were obtained from the EMSL database [34].

3. Results and discussion

3.1. Justification of quantum-chemical approach

In present work B3LYP functional has been applied to obtain reliable molecular structures and vibrational frequencies. CCSD(T) method with additive corrections at MP2 and SODFT levels have been used in order to calculate reaction enthalpies and activation barriers.

To illustrate accuracy of our quantum-chemical approach we have calculated the bond dissociation energies (BDEs) for bonds which are formed or broken in the course of reactions under consideration. Experimental and calculated BDEs are listed in Table 1. One can see that our calculated BDEs deviate from experimental values by no more than 1.2 kcal/mol with taking into account experimental uncertainties. So we can suggest that barrier heights and reaction enthalpies to be found can be determined with reasonable accuracy within approach applied.

3.2. Stationary points for substitution reaction coordinate

Substitution reactions under consideration proceed on the triplet potential energy surfaces (PESs). Transition states found in the study of PESs were characterized by single imaginary frequency and intrinsic reaction coordinate (IRC) analysis at B3LYP/AVTZ level. The stationary points on PESs corresponding to reagents and products have only positive frequencies. In Table 2 structure parameters of molecules involved in substitution reactions are presented. The geometry parameters of O_2, CH_3Br and CF_3Br are within good agreement with experimental data also presented in Table 2.

The structures of transition states for substitution reactions (TS) are shown in Fig. 1. Transition states have C–Br bonds elongated as compared with reagents. Fragments CH_3 and CF_3 in $[O_2\cdots CH_3\cdots Br]^{\neq}$ and $[O_2\cdots CF_3\cdots Br]^{\neq}$ are partially inverted as compared with those in CH_3Br and CF_3Br. The O2O1CH1 and O2O1CF1 dihedral angles

Table 1
Comparison of experimental and calculated BDEs (kcal/mol).

Bond	$\Delta E_{CCSD(T)}$[a]	ΔE_{ZPE}[b]	ΔE_{TC}[c]	ΔE_{core}[d]	ΔE_{SR}[e]	ΔE_{SO}[f]	D (0 K)$_{calc}$	D (298 K)$_{calc}$	D (298 K)$_{exp}$	D (298 K)$_{other\ calc}$
$HO_2 \rightarrow H + O_2$	53.86	−6.51	−5.34	0.11	−0.11	0.00	47.4	48.5	49.16 ± 0.06[g]	
$CH_3Br \rightarrow CH_2Br + H$	107.73	−9.42	−7.60	0.09	0.11	0.00	98.5	100.3	102.1 ± 0.6[g]	
$CH_3Br \rightarrow CH_3 + Br$	76.77	−4.59	−3.15	0.31	−0.53	−3.51	68.4	69.9	70.3 ± 0.5[g]	
$CH_3O_2 \rightarrow CH_3 + O_2$	35.45	−5.86	−4.30	0.11	−0.12	0.00	29.6	31.1	32.7 ± 0.9[g]	
$CF_3Br \rightarrow CF_3 + Br$	74.66	−1.35	−0.59	0.15	−0.19	−3.51	69.8	70.5	70.8 ± 0.3[g]	71.4[i]
$CF_3O_2 \rightarrow CF_3 + O_2$	41.42	−2.67	−1.67	0.10	−0.10	0.00	38.7	39.7	34.2 ± 4.8[h]	40.4[g,j]

[a] Electron correlation energy computed at CCSD(T)/AVTZ//B3LYP/AVTZ level.
[b] Zero-point energies calculated at B3LYP/AVTZ level.
[c] Thermal correction to the enthalpy calculated at B3LYP/AVTZ level.
[d] Core–valence and core–core correlation corrections were obtained as difference between MP2(ae)/cc-pwCVTZ and MP2(fc)/cc-pwCVTZ energies at B3LYP/AVTZ geometries. In MP2 calculations AVTZ basis set was used on hydrogen.
[e] Scalar relativistic corrections were estimated as difference between MP2(DKH)/VTZ-DK and MP2/VTZ energies at B3LYP/AVTZ geometries.
[f] Experimental spin–orbit splitting for atomic bromine was taken from [31].
[g] Recommended values from Ref. [35].
[h] Ref. [36].
[i] Ref. [37], the estimated value at the CBS limit plus contributions from including the core electrons, relativistic and spin–orbit contributions.
[j] Ref. [38], value from G3MP2B3 calculations.

Table 2
Geometries of species from substitution reactions calculated at B3LYP/AVTZ level (experimental values are given in braces).

Species	Symmetry	Bond distance (Å)	Valence angle (°)	Dihedral angle (°)
O_2	$D_{\infty h}$	r(OO) = 1.206 {r(OO) = 1.2075}[a]		
CH_3Br	C_{3v}	r(CBr) = 1.960, r(CH) = 1.083 {r(CBr) = 1.934, r(CH) = 1.0825}[b]	φ(HCH) = 111.23 {φ(HCH) = 111.17}[b]	
CH_3O_2[c]	C_s	r(CH2) = 1.088, r(CH1) = 1.087, r(CO1) = 1.448, r(O1O2) = 1.317	φ(O2O1C) = 111.4, φ(O1CH1) = 105.5, φ(O1CH2) = 109.0	θ(O2O1CH1) = 180.0
$[O_2\cdots CH_3\cdots Br]^{\neq}$	C_s	r(CBr) = 2.629, r(CH2) = 1.077, r(CH1) = 1.078, r(CO1) = 1.746, r(O1O2) = 1.245	φ(O2O1C) = 114.4, φ(O1CH1) = 97.0, φ(O1CH2) = 98.8, φ(O1CBr) = 179.3, φ(BrCH1) = 82.3, φ(BrCH2) = 81.5	θ(O2O1CH1) = 180.0
CF_3Br	C_{3v}	r(CBr) = 1.949, r(CF) = 1.330 {r(CBr) = 1.923, r(CF) = 1.326}[d]	φ(FCF) = 108.73 {φ(FCF) = 108.8}[d]	
CF_3O_2[c]	C_s	r(CF2) = 1.322, r(CF1) = 1.322, r(CO1) = 1.429, r(O1O2) = 1.324	φ(O2O1C) = 110.6, φ(O1CF1) = 105.1, φ(O1CF2) = 110.6	θ(O2O1CF1) = 180.0
$[O_2\cdots CF_3\cdots Br]^{\neq}$	C_s	r(CBr) = 2.897, r(CF2) = 1.271, r(CF1) = 1.274, r(CO1) = 2.071, r(O1O2) = 1.232	φ(O2O1C) = 113.2, φ(O1CF1) = 93.2, φ(O1CF2) = 92.6, φ(O1CBr) = 177.9, φ(BrCF1) = 89.0, φ(BrCF2) = 86.3	θ(O2O1CF1) = 0.0

[a] Ref. [39].
[b] Ref. [40].
[c] Atomic numbers denoted as in corresponding transition states.
[d] Ref. [41].

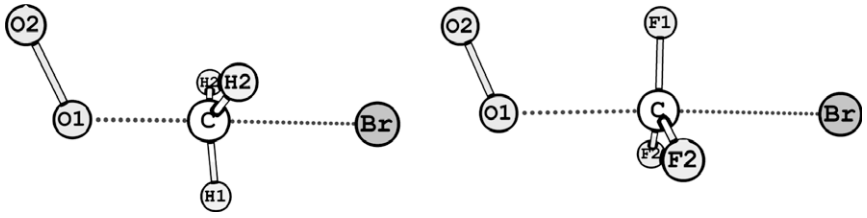

Fig. 1. Structures of the transition states for the "inversion substitution" reactions $CX_3Br + O_2 \rightarrow CX_3O_2 + Br$ (X = H, F).

are 180° both in CH_3O_2 and CF_3O_2 molecules, but they are not identical in corresponding TSs (180° and 0°, respectively). The O1CBr angles differ slightly from 180° and are equal to 179.3° in $[O_2\cdots CH_3\cdots Br]^{\neq}$ and 177.9° in $[O_2\cdots CF_3\cdots Br]^{\neq}$.

Computed vibrational frequencies and rotational constants for species involved are summarized in Table 3. The results of calculations are in a good agreement with available experimental data also presented in Table 3.

3.3. Energy barriers and enthalpy values

We have computed activation barriers and reaction enthalpies for bimolecular reactions proceeding by both substitution mechanism

$$CX_3Br + O_2 \rightarrow CX_3O_2 + Br (X = H, F) \quad (3)$$

and H-abstraction mechanism for CH_3Br

$$CH_3Br + O_2 \rightarrow CH_2Br + HO_2 \quad (4)$$

as well as for unimolecular decay of CF_3Br

$$CF_3Br \rightarrow CF_3 + Br \quad (5)$$

These results are shown in Fig. 2. We do not consider the F-abstraction reaction $CF_3Br + O_2 \rightarrow CF_2Br + FO_2$ because its very high endoergicity of $\Delta H^{O}_{298} = 107.5 \pm 5.5$ kcal/mol as calculated on the basis of data from the Handbook [35] makes it noncompetitive with reactions (3) and (5).

The activation barriers for reactions (4) and (5) were found to be equal to corresponding enthalpies since B3LYP calculation shows

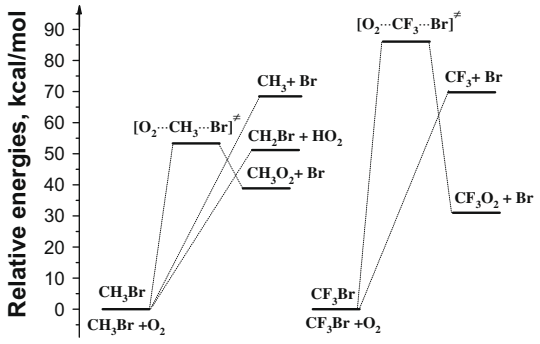

Fig. 2. The energy diagram for the "inversion substitution" $CX_3Br + O_2 \rightarrow CX_3O_2 + Br$ (X = H, F), H-abstraction $CH_3Br + O_2 \rightarrow CH_2Br + HO_2$ and dissociation $CX_3Br \rightarrow CX_3 + Br$ (X=H, F) reactions.

no saddle points for them. In the work of Lee et al. [37] transition state for reaction (5) was located on the singlet PES by *ab initio* calculations and was found to be slightly higher in energy as compared with corresponding products, but our B3LYP calculation does not reveal any saddle point on the reaction coordinate for the process (5). For H-abstraction reaction in methane [47] similar to the process (4) no transition state was also found with B3LYP though it was revealed with other methods. It was located to be slightly lower in energy relative to the reaction products. These literature data show that barrier height for these reactions can slightly deviate from endoergicity. But the detailed study of H-abstraction reaction (4) and unimolecular decay (5) are beyond the scope of the current work. So we have used calculated enthalpies for these reactions to estimate the energy barrier height.

Due to spin–orbit coupling in open-shell TSs the activation barrier for reactions (3) is reduced. We have evaluated this effect with assumption that the main contribution to the spin–orbit coupling is governed by partially bounded bromine. In order to obtain spin–orbit correction, SODFT method was used with RECP on bromine only. REP and AREP computations were made on nonrelativistic B3LYP/AVTZ geometries of TSs (single-point calculations) as well as on reoptimized ones. The changes of TSs structures due to relativistic effects are not essential as indicated by negligible corresponding changes in spin–orbit coupling values presented in Table 4. Therefore, we will consider influence of spin–orbit coupling only on energy but not on geometry and other molecular properties of TSs. Spin–orbit coupling in $[O_2\cdots CF_3\cdots Br]^{\neq}$ is more than that in $[O_2\cdots CH_3\cdots Br]^{\neq}$ because of longer C–Br distance.

Enthalpies and activation barriers for reactions (3)–(5) and reverse to (3) are presented in Table 5. For comparison in this table the experimental values of reaction enthalpies are also presented. For the process $CH_3O_2 + Br \rightarrow CH_3Br + O_2$ the recent results of enthalpy and activation barrier calculations by Francisco and Crowley [48] are also given. In calculations of paper [48] CCSD(T)/6-311++G(2df,2p)//B3LYP/6-31G(d) and QCISD(T)/6-311++G(2df,-2p)//B3LYP/6-31G(d) approaches have been utilized and geometric average of these two results are used by these authors as the estimates of calculated parameters. The most important difference of the approach applied in our work for calculations of energy as compared with that of paper [48] is the use of extra energy corrections at MP2 and SODFT levels in our work. Probably these corrections are responsible for better agreement with experiment of reaction enthalpy calculated in this work. Here we should also comment the high uncertainty of the experimental enthalpy values presented in Table 5 as well as in Table 1 for the processes involving the radical CF_3O_2. To calculate the enthalpy of these processes the estimate of CF_3–O_2 bond energy made by Vedeneev et al. [36] has been used. This estimate was obtained on the basis of comparison of experimentally measured pressure dependence of the rate constant for recombination $CF_3 + O_2(+M) \rightarrow CF_3O_2(+M)$ with dependence calculated within RRKM theory. The weak dependence of calculated rate constant on this bond energy is the reason of high uncertainty of the estimate obtained.

The results of calculations presented in Table 5 show that in the case of CF_3Br the barrier for substitution reaction (3) is higher than that for unimolecular decay of CF_3Br by about 15 kcal/mol. This means that oxygen assisted substitution (3) can be neglected from the list of processes governing the lifetime of CF_3Br under combustion conditions. For CH_3Br molecule the activation barrier of substitution mechanism is lower than that for unimolecular decay by 15.1 kcal/mol. The ratio of the rates of bimolecular substitution (3) and unimolecular decay (5) depend on concentration of oxygen and temperature. As far as competition of substitution (3) with another bimolecular process of H-abstraction (4) is concerned the barrier for substitution exceeds that for the H-abstraction reaction by only 2.1 kcal/mol. This means that this "inversion substitution" should be considered as a competing process in the interaction of oxygen with CH_3Br.

It is worth comparing the barriers for "inversion substitution" for two different substrates CH_3Br and CF_3Br. For the fluorosubstituted bromomethane CF_3Br the barrier is higher by about 33 kcal/mol (Table 5). We attribute this difference to the difference in the barrier heights for the inversion of CF_3 and CH_3 groups. The barrier for the inversion of free CF_3 radical was calculated by Harding to be of 32.6 kcal/mol and for CH_3 the barrier is equal to 0 [49]. The equality of this difference with difference in activation energy barrier is probably accidental. But the essential coupling of reaction coordinate of "inversion substitution" with methyl group inversion in the region of barrier was revealed earlier after the analysis of the reaction coordinate for the example system $SiH_3I + O_2 \rightarrow SiH_3O_2 + I$ [6].

For the same inverting group we can expect the applicability of Evans–Polanyi type correlation $E_0 = \gamma + \delta \cdot \Delta H_0^O$ between activation barrier (E_0) and enthalpy (ΔH_0^O) of substitution reactions for substrates with various leaving groups X. For the reactions of the type $CH_3X + O_2 \rightarrow CH_3O_2 + X$ we have build this correlation which is presented in Fig. 3. For this correlation we have used the calculated data of this work for X = Br and earlier calculated results for X = H [5] and for X = I [6]. This correlation allows one to estimate approximately the possible role of "inversion substitution" reactions with oxygen for other substrates of CH_3X type. We can estimate the barrier height for the substitution reactions with other halogen atoms as the leaving group X. For this estimate the data on formation enthalpies ΔH_{298}^O for reagents and products of substitution $CH_3X + O_2 \rightarrow CH_3O_2 + X$ have been taken from the Handbook [35]. These values and vibrational frequencies for O_2 [39], CH_3O_2

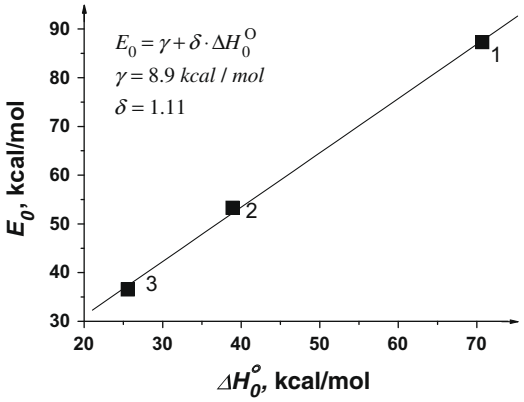

Fig. 3. Linear correlation between the activation barrier E_0 and reaction enthalpy ΔH_0^O for "inversion substitution" reactions of the type $CH_3X + O_2 \rightarrow CH_3O_2 + X$ for different leaving groups X with points 1(X = H), 2(X = Br) and 3(X = I).

Table 3
Rotational constants and vibrational wavenumbers of species from the substitution reactions calculated at the B3LYP/AVTZ level (experimental values are given in braces).

Species	Rotational constants (cm^{-1})	Vibrational wavenumbers (cm^{-1})
O_2	1.450	1626 {1580}[a]
CH_3Br	5.231, 0.314(2)	589 {611}[b], 963(2) {955(2)}[b], 1328 {1306}[b], 1476(2) {1443(2)}[b], 3082 {2935}[b], 3185(2) {3056(2)}[b]
CH_3O_2	1.765, 0.376, 0.330	131 {170 ± 8}[c], 490 {482 ± 9}[d], 910 {902}[e], 1127 {1117 ± 2}[c], 1150 {1183}[c], 1216, 1441 {1408}[c], 1473 {1441}[c], 1483 {1453 ± 2}[c], 3050 {2954} [c], 3138 {3020 ± 2}[c], 3151 {3033}[c]
$[O_2\cdots CH_3\cdots Br]^{\neq}$	1.239, 0.0323, 0.0317	640i, 90, 112, 160, 177, 424, 1003, 1036, 1144, 1359, 1419, 1422, 3122, 3292, 3294
CF_3Br	0.190, 0.068(2)	298(2) {306(2)}[b], 336 {349}[b], 542(2) {547(2)}[b], 751 {760}[b], 1056 {1089}[b], 1181(2) {1210(2)}[b]
CF_3O_2	0.186, 0.108, 0.107	109, 277 {289.6}[f], 411 {402.7}[f], 442 {449.6}[f], 568 {495.0}[f], 586 {596.9}[f], 692 {694.8}[f], 857 {872.7}[f], 1092 {1099.6}[f], 1182 {1178.3}[f], 1238 {1266.1}[f], 1283 {1309.0}[f]
$[O_2\cdots CF_3\cdots Br]^{\neq}$	0.163, 0.0224, 0.0221	1087i, 19, 58, 79, 109, 224, 234, 275, 391, 527, 546, 867, 1411, 1497, 1503

[a] Gas, Ref. [39].
[b] Gas, Ref. [42].
[c] Gas, Ref. [43].
[d] Gas, Ref. [44].
[e] Ar matrix, Ref. [45].
[f] Ne matrix, Ref. [46] and references therein (wavenumbers observed in Ar matrix are coincided with Ne matrix values within 7 cm^{-1}).

Table 4
Spin–orbit coupling in transition states (kcal/mol).

Transition state	SODFT//DFT[a]	SODFT[b]
$[O_2\cdots CH_3\cdots Br]^{\neq}$	1.287	1.251
$[O_2\cdots CF_3\cdots Br]^{\neq}$	1.870	1.867

[a] SODFT single-point calculations at nonrelativistic B3LYP/AVTZ geometries.
[b] SODFT calculations at reoptimized geometries.

(Table 3, this work) and CH_3Cl with CH_3F [42] have allowed us to calculate the values $\Delta H_0^O = 51.1$ kcal/mol (X = Cl) and $\Delta H_0^O = 77.3$ kcal/mol (X = F). These values together with correlation presented in Fig. 3 give the values of barrier height for substitution $E_0 = 65.6$ kcal/mol (X = Cl) and $E_0 = 77.3$ kcal/mol (X = F). Taking into account that the barrier of H-abstraction should be much less sensitive to the change of X group we can expect that for the cases of CH_3Cl and CH_3F the H-abstraction will dominate over substitution reaction. For methyl bromide CH_3Br as a substrate the H-abstraction and substitution are competitive. And for the forth member CH_3I of the series the calculated substitution barrier $E_0 = 36.5$ kcal/mol [6] is much lower than the barrier for H-abstraction. So for methyl iodide as a substrate the substitution will dominate over H-abstraction.

3.4. The kinetic parameters for substitution reactions

The rate constants k for substitution reactions (3) were calculated within transition state theory (TST) formalism [50] for the 273÷2000 K temperature range. Then the temperature dependence of the rate constant $k(T)$ was fitted by two expressions:

$$k = A \cdot \left(\frac{T}{1000}\right)^n \cdot e^{-\frac{E_0}{RT}} \tag{6}$$

$$k = A_{arr} \cdot e^{-\frac{E_a}{RT}} \tag{7}$$

and the resulting parameters are presented in Table 6. To calculate rate constant two approaches have been applied. For reaction (3) with both substrates the rigid-rotor-harmonic-oscillator (RRHO) approximation has been utilized to calculate rate constant within transition state theory with the use of the equation

$$k_{\mathrm{RRHO}} = \frac{k_B T}{h} \cdot \frac{Z^{\neq}_{harm}/V}{Z_{O_2,harm}/V \cdot Z_{\mathrm{RX},harm}/V} \cdot e^{-\frac{E_0}{k_B T}} \tag{8}$$

where $Z^{\neq}_{harm}, Z_{O_2,harm}, Z_{RX,harm}$ – harmonic partition functions of transition state and of reagents O_2 and RX. The structure, vibrational wavenumbers and energy barrier values were taken from Tables 3 and 5. The kinetic parameters resulting from the fitting of calculated temperature dependence $k(T)$ are presented for both substitution reactions in Table 6 (lines with RRHO parameters).

Then we have also calculated effect of tunneling and anharmonicity of vibrational degrees of freedom on the rate constant.

Tunneling factor was estimated with the Wigner correction [51] F_{tunnel} (7) ($\nu^{\neq}$ is imaginary vibrational frequency of TS):

$$F_{tunnel}(T) = 1 + \frac{1}{24}\left(\frac{ih\nu^{\neq}}{kT}\right)^2 \tag{9}$$

At $T = 273$ K tunneling factor is equal to 1.47 and 2.37 for RX = CH_3Br and RX = CF_3Br, respectively, but at higher temperatures contribution of tunneling becomes lower.

For the substitution reaction $CH_3Br + O_2 \rightarrow CH_3O_2 + Br$ the calculation of anharmonicity effect on the rate constant has been car-

Table 5
Calculated reaction barrier E_0, enthalpy at 0 K ΔH_0^O and enthalpy at 298 K ΔH_{298}^O (experimental values are given in braces).

Reaction	E_0 (kcal/mol)	ΔH_0^O (kcal/mol)	ΔH_{298}^O (kcal/mol)
$CH_3Br + O_2 \rightarrow CH_3O_2 + Br$	53.3	38.9	38.7 {37.6 ± 1.4}[a]
$CH_3Br + O_2 \rightarrow CH_2Br + HO_2$	51.2	51.2	51.8 {52.94 ± 0.66}[a]
$CH_3Br \rightarrow CH_3 + Br$	68.4	68.4	69.9 {70.3 ± 0.5}[a]
$CF_3Br + O_2 \rightarrow CF_3O_2 + Br$	86.1	31.0	30.8 {36.6 ± 5.1}[a,b]
$CF_3Br \rightarrow CF_3 + Br$	69.8 (71.1)[c]	69.8 (70.6)[c]	70.5 {70.8 ± 0.3}[a] (71.4)[c]
$CH_3O_2 + Br \rightarrow CH_3Br + O_2$	14.5 (10.9)[d]	−38.9 (−42.1)[d]	−38.7 {−37.6 ± 1.4}[a]
$CF_3O_2 + Br \rightarrow CF_3Br + O_2$	55.1	−31.0	−30.8 {−36.6 ± 5.1}[a,b]

[a] Ref. [35].
[b] Ref. [36].
[c] Ref. [37], the estimated values at the CBS limit plus contributions from including the core electrons, relativistic and spin–orbit contributions.
[d] Ref. [48], the geometric average of CCSD(T)/6-311++G(2df,2p)//B3LYP/6-31G(d) and QCISD(T)/6-311++G(2df,2p)//B3LYP/6-31G(d) data.

Table 6
Kinetic parameters of forward and reverse substitution reactions resulted from the fitting $k(T)$ by Eqs. (6) and (7).

Reaction	Variants of TST	A (cm^3/s)	n	E_0 (kcal/mol)	A_{arr} (cm^3/s)	E_a (kcal/mol)
$CH_3Br + O_2 \rightarrow CH_3O_2 + Br$	Rigid rotor-harmonic oscillator (RRHO)	1.3×10^{-11}	2.15	53.3	6.6×10^{-11}	56.0
	RRHO + tunneling + anharmonicity + free rotor	8.4×10^{-12}	1.45	53.3	2.5×10^{-11}	55.1
$CH_3O_2 + Br \rightarrow CH_3Br + O_2$	RRHO	4.8×10^{-12}	1.89	14.5	2.0×10^{-11}	16.8
	RRHO + tunneling + anharmonicity + free rotor	3.1×10^{-12}	1.19	14.5	7.5×10^{-12}	16.0
$CF_3Br + O_2 \rightarrow CF_3O_2 + Br$	RRHO	8.7×10^{-11}	2.56	86.1	6.2×10^{-10}	89.3
	RRHO + tunneling	1.0×10^{-10}	2.19	86.1	5.3×10^{-10}	88.8
$CF_3O_2 + Br \rightarrow CF_3Br + O_2$	RRHO	9.4×10^{-11}	2.38	55.1	6.0×10^{-10}	58.1
	RRHO + tunneling	1.1×10^{-10}	2.01	55.1	5.2×10^{-10}	57.6

ried out with taking into account the deviation of partition functions from harmonic ones for four low-frequency vibrations of transition state (displacement vectors for these normal coordinates are given in Fig. S1). In the transition state $[O_2\cdots CH_3\cdots Br]^{\neq}$ the lowest real vibrational wavenumber of about 90 cm^{-1} (Table 3) belongs to the degree of freedom corresponding to the hindered internal rotation of CH_3 top. The axis of this top is directed very close to C–O1 bond direction (see Fig. 1) with the angle of only 1.2° and to C–Br bond with the angle less than 0.2°. The potential of this rotation fits reasonably well the equation $V = \frac{1}{2}\cdot V_0\cdot(1-\cos\ n\varphi)$ with $n = 3$ and with maximum values taking place for three masked conformations with C–H bond of CH_3 rotor located against O1–O2 bond. The hindrance of this rotation is very small. The calculated barrier differs slightly for masked conformations of $[O_2\cdots CH_3\cdots Br]^{\neq}$ where CH_3 top is rotated by ±60° or 180° as compared with the structure shown in Fig. 1. The calculated barrier values are equal to 0.35 and 0.37 kcal/mol [52], respectively. We have calculated the partition function Z for hindered rotation of symmetrical CH_3 top of C_3 symmetry and barrier $V_0 = 0.37$ kcal/mol within the approach of the rigid frame with attached top by Pitzer and Gwinn [53]. The other numbers used are the moment of inertia A_m of CH_3 top itself and reduced moment of inertia I_m (calculated according to the Eq. (1a) of paper [53]) for rotation of this top in $[O_2\cdots CH_3\cdots Br]^{\neq}$ which are equal to $A_m = 5.7\times10^{-40}$ g cm^2 and $I_m = 4.3\times10^{-40}$ g cm^2, respectively. The comparison of so calculated Z values with the partition function for free rotation $Z_f = (8\pi^3 IkT)^{1/2}/\hbar n$ (n – symmetry number of the top, equal to 3 in our case) shows that the Z_f value overestimates value of Z by only 2% at $T = 300$ K and this difference goes down with raise in temperature. This allows us to neglect the hindrance of internal rotation and to use Z_f as its partition function within all the temperature interval considered.

Next two low frequencies of 112 and 160 cm^{-1} belong to the vibrations of $[O_2\cdots CH_3\cdots Br]^{\neq}$ with bending character and the third one of 177 cm^{-1} has bending character with contribution of symmetric stretching of Br, CH_3 and O_2 subunits. To estimate the effect of anharmonicity on the partition functions of these three vibrations the shape of real potentials has been investigated within B3LYP/AVTZ approach (Fig. S2). The energy of $[O_2\cdots CH_3\cdots Br]^{\neq}$ has been calculated as a function of amplitudes of displacement (q) of atoms from their equilibrium positions. The displacement in any coordinate of any atom can be taken as independent variable. But the energy change is calculated for all atoms participating in the considered normal vibration displaced proportionally according to the shape of corresponding normal coordinate Q (normal-mode-shape-related displacements). So the change in energy with the displacement q corresponds to the change of energy of normal mode when displacement of local coordinate involved is q. All these three potentials were found to be of quadratic–quartic type which fits the equation $V(q) = A\cdot q^2 + B\cdot q^4$. This potential can be presented in the form $V(q) = A\cdot q^2\cdot(1+\alpha\cdot A\cdot q^2)$ with $\alpha = \frac{B}{A^2}$. The coefficient A has been found near the bottom of potential when the contribution of the quartic part is negligible. The coefficient B has been found with larger amplitudes of q and fixed earlier found value of A. When we provide one-normal-mode-shape-related displacements the other normal modes are not excited. So each of these displacements is proportional to the value of corresponding normal coordinate $q\sim Q$. This means that change in potential energy is of quadratic–quartic type against normal coordinate $V(Q) = A'\cdot Q^2 + B'\cdot Q^4$ as well. The energy of normal mode can be presented by equation $E = \frac{\dot{Q}^2}{2} + \frac{\omega^2 Q^2}{2} + \alpha\frac{\omega^4 Q^4}{4}$ with the same α from equation for $V(q)$. We have calculated effect of anharmonicity in classical approximation. Classical partition function for oscillator is equal to $Z = \frac{1}{h}\cdot\int\int e^{-\frac{E(q,p)}{k_BT}}\mathrm{dq}\cdot\mathrm{dp}$, where q and p are the generalized coordinate and impulse which are Q and $\dot{Q}$ in our case. For harmonic oscillator classical partition function is equal to $Z_{harm} = \frac{k_BT}{h\nu}$. For anharmonic oscillator the result is $Z_{anharm} = \frac{k_BT}{h\nu}\cdot\frac{1}{\sqrt{\pi}}\cdot I = Z_{harm}\cdot a$. The integral $I = \int_{-\infty}^{\infty} e^{-x^2\left(1+\alpha k_BTx^2\right)}dx$ with the variable $x = \frac{\omega Q}{\sqrt{2k_BT}}$ has been calculated numerically. For each of three considered oscillators the calculated effect of anharmonicity does not exceed 11% within temperature interval considered. So calculated anharmonicity correction factors a together with quantum harmonic oscillator partition functions have been used to calculate the anharmonic partition functions. Than these three functions and upper discussed Z_f for internal rotor of $[O_2\cdots CH_3\cdots Br]^{\neq}$ were used to calculate the rate constants corrected for anharmonicity and presented in Table 6 for the variant of TST assigned as RRHO + tunneling + anharmonicity + free rotor.

For reaction $CF_3Br + O_2 \rightarrow CF_3O_2 + Br$ all modes were treated in rigid-rotor-harmonic-oscillator (RRHO) approximation because the detailed analysis of the anharmonic potentials in this case would take too much of computer resources.

The Arrhenius preexponential factor A_{arr} and activation energy E_a for substitution reaction $CH_3Br + O_2 \rightarrow CH_3O_2 + Br$ were calculated to be of 2.5×10^{-11} cm^3/s and 55.1 kcal/mol (Table 6), respectively. We have not found any data for Arrhenius parameters for competing bimolecular abstraction reaction $CH_3Br + O_2 \rightarrow CH_2Br + HO_2$ in literature. For estimation of this preexponential factor we can use the value for H-abstraction reaction with other substituted methane. We have used the recommended value of Arrhenius preexponential factor of 3.4×10^{-11} cm^3/s for H-abstraction from methanol [54]. The activation energy E_a for H-abstraction can be estimated to be lower by 2.1 kcal/mol as compared with E_a for substitution reaction. This difference just corresponds to the calculated difference in the barrier E_0 values presented in Table 5. In Fig. 4 the temperature dependence of these rate constants as well as for the rate constant of competing unimolecular decay $CH_3Br \rightarrow CH_3 + Br$ are presented for the temperature interval of 273 ÷ 2000 K. For the last process the Arrhenius parameters from paper [9] have been taken. To compare the rates of unimolecular and bimolecular processes we have considered bimolecular processes of substitution and H-abstraction as the processes of pseudo first order with $k_{eff} = k\cdot[O_2]$, where k is bimolecu-

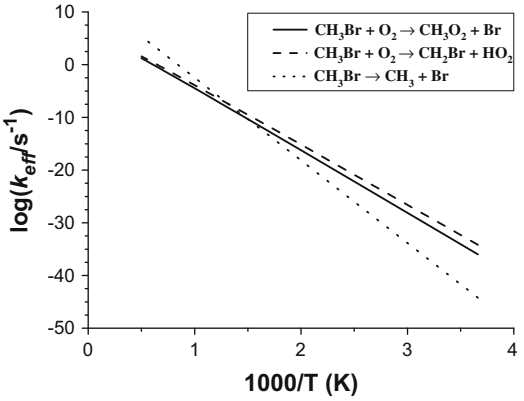

Fig. 4. The temperature dependence of the effective rate constants k_{eff} for the substitution $CH_3Br + O_2 \rightarrow CH_3O_2 + Br$, H-abstraction $CH_3Br + O_2 \rightarrow CH_2Br + HO_2$ and unimolecular decay $CH_3Br \rightarrow CH_3 + Br$ is shown for the temperature interval of 273 ÷ 2000 K. For the bimolecular processes k_{eff} have been calculated as the rate constants of the pseudo first order process $k_{eff} = k\cdot[O_2]$, where k is the rate constant of corresponding bimolecular process. The Arrhenius parameters used are discussed in the text.

lar constant. Taking into account that the kinetic modeling of the flame inhibitor effect is usually carried out for combustion in atmosphere we took the concentration of oxygen to be that in air at corresponding temperature. For unimolecular decay k_{eff} value is equal to unimolecular rate constant. The calculated temperature dependences of the rate constants k_{eff} for all three processes contributing to the initial decomposition of CH_3Br molecule in the conditions of the flame in air are presented in Fig. 4. We see that the unimolecular decay starts to dominate over bimolecular substitution and H-abstraction at temperatures of about 700 K and 760 K, respectively. In the general case of CH_3X substrate the contribution of the substitution reaction can be estimated with the use of correlation between activation barrier height and reaction enthalpy considered above.

4. Conclusion

In this work the computational study of the substitution reactions of two Br-containing fire suppressants with molecular oxygen $CX_3Br + O_2 \rightarrow CX_3O_2 + Br$ (X = H, F) has been carried out. Reaction enthalpies and activation barriers were calculated by DFT and *ab initio* quantum chemical methods including corrections for core, relativistic effects, zero-point vibrational energy. Temperature dependence of the rate constants were calculated within TST formalism in rigid-rotor-harmonic-oscillator approximation with taking into account possible tunneling. For the reaction of lighter substrate the effect of anharmonicity of low-frequency modes has been also considered. For the substrate CF_3Br (Halon-1301) the calculated barrier for substitution reaction is too high which makes the substitution reaction ($CF_3Br + O_2 \rightarrow CF_3O_2 + Br$) noncompetitive as compared with unimolecular decay ($CF_3Br \rightarrow CF_3 + Br$). For methyl bromide the barrier for substitution $CH_3Br + O_2 \rightarrow CH_3O_2 + Br$ is lower than that for unimolecular decay ($CH_3Br \rightarrow CH_3 + Br$) and close in value with barrier for the H-abstraction reaction $CH_3Br + O_2 \rightarrow CH_2Br + HO_2$. This makes substitution reaction competitive with abstraction. The competition of substitution with unimolecular decay of CH_3Br can be estimated for particular experimental conditions (O_2 concentration and temperature) with the use of calculated kinetic parameters. The results of calculations made in this work together with the earlier results have allowed us also to build the correlation of Evans–Polanyi type between the activation barrier and reaction enthalpy for "inversion substitution" reactions $CH_3X + O_2 \rightarrow CH_3O_2 + X$. This correlation can be used for estimation of the role of substitution for substrates CH_3X with other leaving groups X.

Acknowledgments

The financial support of this work by Russian Foundation for Basic Research (Grant No. 09-03-00310-a) is gratefully acknowledged. The computing time on MVS-1000/128 supercomputer was assigned by Institute of Computational Mathematics and Mathematical Geophysics of Siberian Branch of Russian Academy of Sciences.

Appendix A. Supplementary material

Supplementary data associated with this article can be found, in the online version, at doi:10.1016/j.combustflame.2009.11.004.

References

[1] J. Warnatz, in: W.C. Gardiner (Ed.), Combustion Chemistry, Springer-Verlag, New York, 1984, pp. 197–360.
[2] W. Tsang, R.F. Hampson, J. Phys. Chem. Ref. Data 15 (1986) 1087–1279.
[3] D.L. Baulch, C.J. Cobos, R.A. Cox, P. Frank, G. Hayman, T. Just, J.A. Kerr, T. Murrels, M.J. Pilling, J. Troe, R.W. Walker, J. Warnatz, J. Phys. Chem. Ref. Data 23 (1994) 847–1033.
[4] E.T. Denisov, T.G. Denisova, Russ. Chem. Rev. 71 (2002) 417–438.
[5] G.A. Bogdanchikov, A.V. Baklanov, D.H. Parker, Chem. Phys. Lett. 385 (2004) 486–490.
[6] G.A. Bogdanchikov, A.V. Baklanov, D.H. Parker, Russ. Chem. Bull. 57 (2008) 1837–1841.
[7] E.T. Denisov, V.V. Azatyan, Inhibition of Chain Reactions, Gordon and Breach, London, 2000. pp. 1–337.
[8] V. Babushok, W. Tsang, Combust. Flame 123 (2000) 488–506.
[9] V. Babushok, T. Noto, D.R.F. Burgess, A. Hamins, W. Tsang, Combust. Flame 107 (1996) 351–367.
[10] T. Noto, V. Babushok, A. Hamins, W. Tsang, Combust. Flame 112 (1998) 147–160.
[11] Y. Saso, Y. Ogawa, N. Saito, H. Wang, Combust. Flame 118 (1999) 489–499.
[12] Y. Saso, Proc. Combust. Inst. 29 (2002) 337–344.
[13] B.A. Williams, J.W. Fleming, Proc. Combust. Inst. 29 (Part 1) (2002) 345–351.
[14] A.D. Becke, Phys. Rev. A 38 (1988) 3098–3100.
[15] C. Lee, W. Yang, R.G. Parr, Phys. Rev. B 37 (1988) 785–789.
[16] T.H. Dunning Jr., J. Chem. Phys. 90 (1989) 1007–1023.
[17] R.A. Kendall, T.H. Dunning Jr., R.J. Harrison, J. Chem. Phys. 96 (1992) 6796–6806.
[18] A.K. Wilson, D.E. Woon, K.A. Peterson, T.H. Dunning Jr., J. Chem. Phys. 110 (1999) 7667–7676.
[19] C. Møller, M.S. Plesset, Phys. Rev. 46 (1934) 618–622.
[20] G.D. Purvis III, R.J. Bartlett, J. Chem. Phys. 76 (1982) 1910–1918.
[21] K. Raghavachari, G.W. Trucks, J.A. Pople, M. Head-Gordon, Chem. Phys. Lett. 157 (1989) 479–483.
[22] K.A. Peterson, T.H. Dunning Jr., J. Chem. Phys. 117 (2002) 10548–10560.
[23] N.J. DeYonker, K.A. Peterson, A.K. Wilson, J. Phys. Chem. A 111 (2007) 11383–11393.
[24] M. Douglas, N.M. Kroll, Ann. Phys. (NY) 82 (1974) 89–155.
[25] B.A. Hess, Phys. Rev. A 32 (1985) 756–763.
[26] B.A. Hess, Phys. Rev. A 33 (1986) 3742–3748.
[27] W.A. de Jong, R.J. Harrison, D.A. Dixon, J. Chem. Phys. 114 (2001) 48–53.
[28] Y.S. Lee, in: P. Schwerdtfeger (Ed.), Relativistic Electronic Structure Theory, Part 2: Applications, Elsevier, Amsterdam, 2004, pp. 352–416.
[29] M.M. Hurley, L.F. Pacios, P.A. Christiansen, R.B. Ross, W.C. Ermler, J. Chem. Phys. 84 (1986) 6840–6853.
[30] H.S. Lee, W.K. Cho, Y.J. Choi, Y.S. Lee, Chem. Phys. 311 (2005) 121–127.
[31] C.E. Moore, Atomic Energy Levels, vol. III, US Government Printing Office, Washington, DC, 1959.
[32] E.J. Bylaska, W.A. de Jong, N. Govind, K. Kowalski, T.P. Straatsma, M. Valiev, D. Wang, E. Apra, T.L. Windus, J. Hammond, P. Nichols, S. Hirata, M.T. Hackler, Y. Zhao, P.-D. Fan, R.J. Harrison, M. Dupuis, D.M.A. Smith, J. Nieplocha, V. Tipparaju, M. Krishnan, Q. Wu, T. Van Voorhis, A.A. Auer, M. Nooijen, E. Brown, G. Cisneros, G.I. Fann, H. Fruchtl, J. Garza, K. Hirao, R. Kendall, J.A. Nichols, K. Tsemekhman, K. Wolinski, J. Anchell, D. Bernholdt, P. Borowski, T. Clark, D. Clerc, H. Dachsel, M. Deegan, K. Dyall, D. Elwood, E. Glendening, M. Gutowski, A. Hess, J. Jaffe, B. Johnson, J. Ju, R. Kobayashi, R. Kutteh, Z. Lin, R. Littlefield, X. Long, B. Meng, T. Nakajima, S. Niu, L. Pollack, M. Rosing, G. Sandrone, M. Stave, H. Taylor, G. Thomas, J. van Lenthe, A. Wong, Z. Zhang, NWChem, A Computational Chemistry Package for Parallel Computers, Version 5.1, Pacific Northwest National Laboratory, Richland, WA, USA, 2007.
[33] M.J. Frisch, G.W. Trucks, H.B. Schlegel, G.E. Scuseria, M.A. Robb, J.R. Cheeseman, J.A. Montgomery Jr., T. Vreven, K.N. Kudin, J.C. Burant, J.M. Millam, S.S. Iyengar, J. Tomasi, V. Barone, B. Mennucci, M. Cossi, G. Scalmani, N. Rega, G.A.

Petersson, H. Nakatsuji, M. Hada, M. Ehara, K. Toyota, R. Fukuda, J. Hasegawa, M. Ishida, T. Nakajima, Y. Honda, O. Kitao, H. Nakai, M. Klene, X. Li, J.E. Knox, H.P. Hratchian, J.B. Cross, C. Adamo, J. Jaramillo, R. Gomperts, R.E. Stratmann, O. Yazyev, A.J. Austin, R. Cammi, C. Pomelli, J.W. Ochterski, P.Y. Ayala, K. Morokuma, G.A. Voth, P. Salvador, J.J. Dannenberg, V.G. Zakrzewski, S. Dapprich, A.D. Daniels, M.C. Strain, O. Farkas, D.K. Malick, A.D. Rabuck, K. Raghavachari, J.B. Foresman, J.V. Ortiz, Q. Cui, A.G. Baboul, S. Clifford, J. Cioslowski, B.B. Stefanov, G. Liu, A. Liashenko, P. Piskorz, I. Komaromi, R.L. Martin, D.J. Fox, T. Keith, M.A. Al-Laham, C.Y. Peng, A. Nanayakkara, M. Challacombe, P.M.W. Gill, B. Johnson, W. Chen, M.W. Wong, C. Gonzalez, J.A. Pople, Gaussian 03, Revision C.02, Gaussian, Inc., Wallingford, CT, 2004.

[34] EMSL basis set library. <http://www.emsl.pnl.gov/forms/basisform.html>.

[35] Y.-R. Luo, Comprehensive Handbook of Chemical Bond Energies, CRC Press, Taylor and Francis Group, Boca Raton, FL, 2007.

[36] V.I. Vedeneev, M.Y. Goldenberg, M.A. Teitelboim, Kinet. Katal. 28 (1987) 156–159.

[37] E.P.F. Lee, J.M. Dyke, F.-T. Chau, W.-K. Chow, D.K.W. Mok, Chem. Phys. Lett. 376 (2003) 465–474.

[38] R. Janoschek, M.J. Rossi, Int. J. Chem. Kinet. 36 (2004) 661–686.

[39] K.P. Huber, G. Herzberg, Molecular spectra and molecular structure, Constants of Diatomic Molecules, vol. 4, Van Nostrand Reinhold, New York, 1979.

[40] J. Demaison, L. Margules, J.E. Boggs, Struct. Chem. 14 (2003) 159–174.

[41] V. Typke, M. Dakkouri, H. Oberhammer, J. Mol. Struct. 44 (1978) 85–96.

[42] T. Shimanouchi, J. Phys. Chem. Ref. Data 6 (1972) 993–1102.

[43] D.-R. Huang, L.-K. Chu, Y.-P. Lee, H.-Y. Liao, E.N. Sharp, P. Rupper, T.A. Miller, J. Chem. Phys. 127 (2007) 044311.

[44] S.J. Blanksby, T.M. Ramond, G.E. Davico, M.R. Nimlos, S. Kato, V.M. Bierbaum, W.C. Lineberger, G.B. Ellison, M. Okumura, J. Am. Chem. Soc. 123 (2001) 9585–9596.

[45] S. Nandi, S.J. Blanksby, X. Zhang, M.R. Nimlos, D.C. Dayton, G.B. Ellison, J. Phys. Chem. A 106 (2002) 7547–7556.

[46] S. Sander, H. Pernice, H. Willner, Chem. Eur. J. 6 (2000) 3645–3653.

[47] N.K. Srinivasan, J.V. Michael, L.B. Harding, S.J. Klippenstein, Combust. Flame 149 (2007) 104–111.

[48] J.S. Francisco, J.N. Crowley, J. Phys. Chem. A 110 (2006) 3778–3784.

[49] L.B. Harding, Ber. Bunsen-Ges. Phys. Chem. 101 (1997) 363–371.

[50] E.E. Nikitin, Theory of Elementary Atomic and Molecular Processes in Gases, Claredon Press, Oxford, UK, 1974.

[51] E.P. Wigner, Z. Phys. Chem. B19 (1932) 203–216.

[52] Energy differences were calculated within introduced approach (see Computational Details) excluding ZPE. Single-point calculations were made for masked conformations. Spin–orbit correction was assumed to be the same for all structures.

[53] K.S. Pitzer, W.D. Gwinn, J. Chem. Phys. 10 (1942) 428–440.

[54] W. Tsang, J. Phys. Chem. Ref. Data 16 (1987) 471–508.